Clouds over soot evaporation: errors in modeling laser-induced incandescence of soot

Smallwood, Gregory; Snelling, David; Liu, Fengshan; Gulder, Omar L.

Publisher's version / Version de l'éditeur:
https://doi.org/10.1115/1.1370507
Journal of Heat Transfer, 123, August 4, pp. 814-818, 2001

MARIA CLANCY
DGO
INST FOR CHEM PROCESS & ENVIR TECH
NATIONAL RESEARCH COUNCIL CANADA
M-12, ROOM 141, 1200 MONTREAL RD.
OTTAWA, ON K1A 0R6
CANADA

Acknowledgment

The financial support of this research by the National Science Council under the contract NSC 87-2212-E-211-006 is greatly appreciated.

Nomenclature

a, b = width and height of a rectangular duct, respectively
D_e = equivalent hydraulic diameter, $2ab/(a+b)$, m
I, J = number of finite difference divisions in the X and Y directions, respectively
n = dimensionless outward normal direction to the wall
Ra^* = modified Rayleigh number, Racos δ
Re_w = wall Reynolds number, $v_{in}D_e/\nu$
v_{in} = magnitude of fluid velocity injected or suctioned through the porous walls
X, Y, Z = dimensionless rectangular coordinate, $X=x/D_e$, $Y=y/D_e$, $Z=z/(\mathrm{Re}\,D_e)$
Z^* = dimensionless z-direction coordinate, $z/(\mathrm{Pr}\,\mathrm{Re}\,D_e)=Z/\mathrm{Pr}$

Greek Symbols

δ = duct inclination angle
Δ = mixed convection parameter, $(\mathrm{Ra}/\mathrm{Re})\sin\delta$
γ = aspect ratio of a rectangular duct, a/b
ξ = dimensionless vorticity in axial direction

Subscripts

b = bulk fluid quantity
o = value at inlet
w = value at wall

Superscripts

$-$ = average value

References

[1] Cheng, K. C., and Hong, S. W., 1972, "Effect of Tube Inclination on Laminar Convection in Uniformly Heated Tubes for Flat-Plate Solar Collectors," Sol. Energy, **13**, pp. 363–371.
[2] Sabbagh, J. A., Aziz, A., El-Aring, A. S., and Hamad, G., 1976, "Combined Free and Forced Convection Heat Transfer in Inclined Circular Tubes," ASME J. Heat Transfer, **98**, pp. 322–324.
[3] Abdelmeguid, A. M., and Spalding, D. B., 1979, "Turbulent Flow and Heat Transfer in Pipes With Buoyancy Effects," J. Fluid Mech., **94**, Part 2, pp. 383–400.
[4] Morcos, E. M., and Abou-Ellail, M. M. M., 1983, "Buoyancy Effects in the Entrance Region of an Inclined Multirectangular Channel Solar Collector," ASME J. Sol. Energy Eng., **105**, pp. 157–162.
[5] Cheng, K. C., and Yuen, F. P., 1985, "Flow Visualization Studies on Secondary Flow Pattern for Mixed Convection in the Entrance Region of Isothermally Heated Inclined Pipes, Fundamentals of Forced and Mixed Convection," ASME HTD, **42**, pp. 121–130.
[6] Morcos, S. M., Hilal, M. M., Kamel, M. M., and Soliman, M. S., 1986, "Experimental Investigation of Mixed Laminar Convection in the Entrance Region of Inclined Rectangular Channels," ASME J. Heat Transfer, **108**, pp. 574–579.
[7] Choudhury, D., and Patankar, S. V., 1988, "Combined Forced and Free Laminar Convection in the Entrance Region of an Inclined Isothermal Tube," ASME J. Heat Transfer, **110**, pp. 901–909.
[8] Olson, R. M., and Eckert, E. R. G., 1966, "Experimental Studies of Turbulent Flow in a Porous Circular Tube With Uniform Fluid Injection Through the Tube Wall," ASME J. Appl. Mech., **33**, pp. 7–17.
[9] Yuan, S. W., and Finkelstein, A. B., 1958, "Heat Transfer in Laminar Pipe Flow With Uniform Coolant Injection," Jet Propul., **28**, pp. 178–181.
[10] Pederson, R. J., and Kinney, R. B., 1971, "Entrance-Region Heat Transfer for Laminar Flow in Porous Tubes," Int. J. Heat Mass Transf., **14**, pp. 159–161.
[11] Raithby, G. D., 1971, "Laminar Heat Transfer in the Thermal Entrance of Circular Tubes and Two-Dimensional Rectangular Ducts With Wall Suction and Injection," Int. J. Heat Mass Transf., **14**, pp. 224–243.
[12] Hirata, Y. S., Hirata, Y. S., and Ito, R., 1982, "Experimental Study of Flow Development in a Porous Tube With Injection or Suction," J. Chem. Eng. Jpn., **15**, pp. 455–451.
[13] Kinney, R. B., 1968, "Fully Development Frictional and Heat Transfer Characteristics of Laminar Flow in Porous Tubes," Int. J. Heat Mass Transf., **11**, pp. 1393–1401.
[14] Hwang, G. J., Cheng, Y. C., and Ng, M. L., 1993, "Developing Laminar Flow and Heat Transfer in a Square Duct With One-Walled Injection and Suction," Int. J. Heat Mass Transf., **36**, pp. 2429–2440.
[15] Cheng, Y. C., and Hwang, G. J., 1995, "Experimental Study of Laminar Flow and Heat Transfer in a One-Porous-Wall Square Duct With Wall Injection," Int. J. Heat Mass Transf., **38**, pp. 3475–3484.
[16] Lee, K. T., and Yan, W. M., 1998, "Mixed Convection Heat Transfer in Horizontal Rectangular Ducts With Wall Transpiration Effects," Int. J. Heat Mass Transf., **41**, pp. 411–423.
[17] Ramakrishna, K., Rubin, S. G., and Khosla, P. K., 1982, "Laminar Natural Convection Along Vertical Square Ducts," Numer. Heat Transfer, **5**, pp. 59–79.
[18] Shah, R. A., and London, A. L., 1978, *Laminar Flow Forced Convection in Ducts*, Spp1. 1 to Adv. Heat Transfer, Academic Press, New York, pp. 196–222.

Clouds Over Soot Evaporation: Errors in Modeling Laser-Induced Incandescence of Soot

G. J. Smallwood
Senior Research Officer
e-mail: greg.smallwood@nrc.ca

D. R. Snelling
Principal Research Officer

F. Liu
Associate Research Officer

Ö. L. Gülder
Senior Research Officer,
Group Leader

Combustion Research Group,
Institute for Chemical Process & Environmental Technology,
National Research Council Canada,
1200 Montreal Road, Ottawa,
Ontario, Canada K1A 0R6

The ambiguity and incorrect treatment of the evaporation term among some LII models in the literature are discussed. This study does not suggest that the correct formulation presented for the evaporation model is adequate, or that it reflects the soot evaporation process under intense evaporation. The emphasis is that the current evaporation model must be used correctly in the evaluation of the LII model against experimental data. Numerical results are presented to demonstrate the significance of the molecular weight associated with the heat of evaporation and the thermal velocity of carbon vapor on the results obtained with the evaporation model. Other errors frequently repeated in the literature are also identified. [DOI: 10.1115/1.1370507]

Introduction

Laser-induced incandescence (LII) has experienced rapid development as a powerful diagnostic tool for spatially and temporally resolved measurements of soot volume fraction and primary particle size in various applications such as diffusion flames and diesel engine exhaust. The LII technique is based on the detection

Contributed by the Heat Transfer Division for publication in the Journal of Heat Transfer. Manuscript received by the Heat Transfer Division April 3, 2000; revision-received December 7, 2000. Associate Editor: R. Skocypec.

and analysis of the incandescence signals of the enhanced thermal radiation from soot particles subjected to an intense laser pulse. Development of the mathematical model describing the heat and mass transfer processes of LII is not only essential in understanding some aspects of experimental results but it is also useful to improve the capabilities of the technique.

The first effort to model the nanoscale heat and mass transfer processes of soot in LII was made by Eckbreth [1]. Subsequent improvement and application of this model have been presented by Melton [2], Dasch [3], Tait and Greenhalgh [4], Hofeldt [5], and recently by Mewes and Seitzman [6], Snelling et al. [7], McManus et al. [8], Will et al. [9], Snelling et al. [10], and Schraml et al. [11]. Given the assumptions of the current LII model [10], it is not surprising to see some discrepancies between the model predicted and the experimental soot temperatures [11]. The discrepancies found in the study of Schraml et al. are partially attributed to their incorrect treatment of the evaporation heat loss term. Further research and evaluation of the LII model are clearly required. Nevertheless, the usefulness of the current LII model has been demonstrated in several studies [5,8–11]. Central to the LII process is soot evaporation, which reduces the soot particle size and provides an effective cooling mechanism that limits the further rise of soot particle temperature. An adequate treatment of the evaporation term is the key to the success of an LII model to predict the time-resolved soot particle size, soot temperature, and the excitation curve. Unfortunately, significant differences exist in the treatment of the vaporization heat loss term among the LII models found in the literature. Our research revealed that the ambiguity, confusion, and incorrect treatment of the soot evaporation term originated in the first LII modeling paper by Eckbreth [1]. The incorrect formulation has been widely spread in the growing community of LII modeling [2,4,9], although the correct formulation of the soot evaporation model was given by Dasch [3] and Hofeldt [5]. The present paper is motivated by the pressing need to clarify the confusion and incorrect treatment of the soot evaporation model among some researchers working on LII modeling. The objectives of this study are (1) to clarify the confusion surrounding the soot evaporation model and establish the correct formulation in order to prevent further use of the incorrect one, and (2) to numerically evaluate the impact of using the incorrect soot evaporation model.

Evaporation Models

A detailed description of the LII model employed in this study has been given by Snelling et al. [10] and therefore is not repeated here. The energy balance equation is given here for the convenience of the reader.

$$C_a q - \frac{2k_a(T-T_g)\pi d_p^2}{(d_p+G\lambda_{\mathrm{MFP}})} + \frac{\Delta H_v(T)}{M_v(T)}\frac{dM}{dt} + q_{\mathrm{rad}} = \frac{1}{6}\pi d_p^3 \rho_s c_s \frac{dT}{dt} \tag{1}$$

The terms in Eq. (1) represent, in order, the laser energy absorption by soot particle, heat conduction loss from the soot particle to the surrounding gas in the transition regime, heat loss due to soot evaporation, heat loss through the mechanism of thermal radiation, and finally the rate of soot particle internal energy change. The absorbed laser energy is determined by the laser intensity q, and the absorption cross section $C_a = (\pi^2 d_p^3 E(m))/\lambda$, where d_p is the diameter of the primary particles, $E(m)$ is a refractive index dependent function, and λ is the wavelength of the laser. The parameters in the conduction term include: k_a, the heat conduction coefficient of air; T, the soot temperature; T_g, the gas temperature; d_p, the diameter of the primary particles; G, a geometry-dependent heat transfer factor; and λ_{MFP}, the mean free path. The parameters in the evaporation term are: $\Delta H_v(T)$, the particle temperature dependent heat of evaporation of graphite; $M_v(T)$, the particle temperature dependent molecular weight of soot vapor; M, the mass of soot particle; and t is time. q_{rad} is the heat loss term due to radiation. Additional parameters presented in the internal energy term are: ρ_s, the density of soot; and c_s, the specific heat of soot.

To illustrate the differences in the treatment of the evaporation heat loss term between the present LII model and the models presented and/or employed by others, these evaporation models are compared in Table 1, where β is the evaporation coefficient, $P_v(T)$ is the particle temperature dependent vapor pressure of soot, and R is the universal gas constant.

Except for a minor difference in the introduction of the evaporation coefficient β between Model I and Models II and III, two important differences are observed. First, Model I employs a different molecular weight associated with the heat of vaporization from Models II and III: Model I uses the molecular weight of the soot vapor (M_v) while Models II and III use the molecular weight of the solid carbon (M_s). Secondly, a factor of π is missing from the denominator of the term inside the square root in Model II. It is not clear which expression was used in the studies of Will et al. [9] and Schraml et al. [11] since formulation for dM/dt was not given in their papers. Here we assume that Model III employs the same dM/dt formulation as Model I.

It is understandable to easily make incorrect use of the molecular weight associated with the heat of vaporization if careful thought is not given to the physical situation of soot (assuming graphite) evaporation. It is well known that multiple species of carbon coexist in the vapor with C_3 as the most abundant species based on the thermodynamic equilibrium calculations of Leider et al. [12]. In addition, the heat of evaporation, ΔH_v, is the energy required to evaporate unit mole solid carbon into multiple gaseous carbon species. Therefore, the mean molecular weight of the vapor should be used, not the molecular weight of the solid carbon, so that the heat of evaporation is consistent with the molecular weight. Certainly, it would be correct to use the molecular weight of solid carbon if only a single species (C_1) exists in the vapor, or if ΔH_v corresponding to C_1 only is used. A temperature

Table 1 Comparison of the evaporation models in the literature

Model I	Model II	Model III
Present study Dasch[a] [3] Hofeldt [5]	Eckbreth [1] Melton [2] Tait and Greenhalgh[b] [4]	Will et al.[c] [9] Schraml et al.[c] [11]
$-\frac{\Delta H_v}{M_v}\pi d_p^2 \beta P_v(T)\sqrt{\frac{M_v}{2\pi RT}}$	$-\frac{\Delta H_v}{M_s}\pi d_p^2 P_v(T)\sqrt{\frac{M_v}{2RT}}$	$\frac{\Delta H_v}{M_s}\frac{dM}{dt}$

[a]Dasch [3] did not use the evaporation coefficient β.

[b]The square root term was given as $\sqrt{\frac{M_v}{2}RT}$, which is likely to be a typo.

[c]Will et al. [9] and Schraml et al. [11] did not present their expressions for dM/dt.

dependent mean molecular weight is used in the numerical model, rising from 24 at 2000 K to 36 at 3600 K to 48 at 4700 K. Thus the error in using C_1, with a molecular weight of 12, increases from overestimating the enthalpy loss from soot mass evaporation by a factor of 2 at 2000 K to a factor of 4 at 4700 K.

As for the second difference associated with the thermal velocity of vapor between Model I and Model II, it is emphasized here that the expression of Model I is correct. A detailed derivation of the mass flux of vapor that crosses unit area toward one side was given by Kennard [13] and is written as

$$\Phi = P_v \sqrt{\frac{M_v}{2\pi RT}}. \tag{2}$$

Application of Eq. (2) to calculate the evaporation heat loss term leads to the expression of Model I given in Table 1. The rationale of introducing an evaporation coefficient, β, has been discussed by Kennard [13]. The evaporation heat loss term of Model II given in Table 1 implies that the mass flux of vapor would read

$$\Phi' = P_v \sqrt{\frac{M_v}{2RT}} \tag{3}$$

resulting in a predicted enthalpy loss that is 1.8 times too high. The combination of the inconsistent use of molecular weights and the incorrect formulation for the mass flux of vapor presented in Model II produces an overall predicted enthalpy loss that ranges from 3.6 times too high at 2000 K to 7.2 times too high at 4700 K.

Such overestimations of the enthalpy losses are anticipated to cause the particle temperatures to be much cooler and the evaporated mass loss to be much less with Models II and III in comparison with Model I.

In addition to the confusion and incorrect treatment regarding the evaporation term of the LII models in the literature, it is also worth pointing out that Melton [2] gave an incorrect expression for the thermal conductivity of air, which has been previously identified [6]. According to Melton, the thermal conductivity of air was calculated as $K_a = 5.83\times10^{-5}(T/273)^{0.82}$ W cm^{-1} K^{-1} based on the expression given by Tsederberg [14]. It was noticed by Mewes and Seitzman [6] that this expression yields air thermal conductivity that is only about one fourth of well-established values. After consulting the expression given by Tsederberg, it was realized that Melton [2] neglected to convert calorie to joule in the expression shown above, thus accounting for the discrepancy. In addition, the analytical expression for the thermal conductivity of air given in Tsederberg is applicable only up to 1273 K. Therefore, neither the expression given in Melton nor the expression given in Tsederberg should be employed in LII modeling since temperatures in a flame are well above the upper temperature limit of the expression given in Tsederberg. On the other hand, one should be aware that use of the thermal conductivity of air in modeling the heat conduction term is only an approximation, since the local thermal conductivity of combustion gas varies significantly in a flame and in the exhaust gases due to variations in the composition.

Furthermore, there is a typographical error in Melton [2] in the sign of the exponent for the heat of vaporization of carbon, which should have read $7.78\times10^{+5}$ J/mol.

Results and Discussion

Characteristics of the excitation laser were given in detail in Snelling et al. [10]. Briefly, the wavelength of the laser is 532 nm and it has a typical Q-switched temporal profile of 7 ns FWHM duration. The spatial profile of the laser intensity is top-hat (uniform). The primary soot particle size assumed in the calculations is 32 nm. Unless otherwise stated, the evaporation coefficient β is assumed to be 1.0. $E(m)$ based on the refractive index of soot due to Lee and Tien [15] (0.176 at 532 nm) was used in all the calculations. The numerical solver uses an adaptive fourth-order Runge-Kutta algorithm that optimizes the step size to minimize the truncation error. The numerical results discussed below were obtained using a time step of 0.25 ns. Investigations were performed to ensure that this time step was sufficiently small to achieve results independent of the time step, with maximum deviation of less than 0.1 percent. Effects of using the three different evaporation models given in Table 1 on the model predictions were investigated.

The physical properties used in the present calculations are specified as follows. The local gas temperature $T_g = 1800$ K, a typical value found in flames. The corresponding values of k_a, G, and λ_{MFP} are 0.12 W/m K, 22.064, and 0.5665 μm, respectively. The soot density and specific heat are taken at the values of local gas temperature, i.e., $\rho_s = 2.2$ g/cm^3 [12] and $c_s = 2.1$ J/g K [16] since they only vary mildly with temperature. Properties related to the soot evaporation rate are obtained from the equilibrium calculations of Leider et al. [12] and are given as fifth-order polynomial expressions as $P_v = \exp(\Sigma_{i=0}^{5} p_i T^i)$ atm, $M_v = \Sigma_{i=0}^{5} m_i T^i$ kg/mole, and $\Delta H_v = \Sigma_{i=0}^{5} h_i T^i$ J/K mole. The fitting coefficients are given in Table 2.

When conducting numerical calculations of soot particle size and temperature using the present LII model, it is worth pointing out that there are uncertainties in the predictions due to uncertainties associated with the thermal properties of soot such as the absorption function $E(m)$, the mean molecular weight of soot vapor M_v, the heat of vaporization ΔH_v, the vapor pressure P_v, and input parameters for the heat conduction rate. Based on our best knowledge it was estimated that uncertainties of these properties are well within 30 percent. The effects of the uncertainty in these properties on the numerical predictions were investigated by perturbing the values of the properties discussed above by ±30 percent using Model I at a laser fluence of 0.725 J/cm^2. At this laser fluence, there is significant soot vaporization and properties associated with the heat conduction loss have almost no effect on the solution during and shortly after the laser pulse (the laser pulse duration is 30 ns). Effects of uncertainty of $E(m)$, M_v, ΔH_v, and P_v on the predictions are shown in Fig. 1. Uncertainties in $E(m)$, M_v, and ΔH_v have a significant effect on particle size but have less impact on particle temperature, Figs. 1(*a*), (*b*), and (*c*). Variation of the vapor pressure by 30 percent has a modest effect on the particle temperature and minimal effect on particle size, Fig. 1(*d*). Overall, the uncertainty in the predicted particle temperature and particle size is about 2 percent and 20 percent, respectively.

Effects on the History of Soot Particle Size and Temperature. Calculations were carried out using the three different

Table 2 Fitting coefficients for the vapor pressure, mean molecular weight, and the heat of vaporization

i	p_i	m_i	h_i
0	-122.96	0.017179	205398
1	0.090558	6.8654e-7	736.60
2	-2.7637e-5	2.9962e-9	-0.40713
3	4.1754e-9	-8.5954e-13	1.1992e-4
4	-2.4875e-13	1.0486e-16	-1.7946e-8
5	0.0	0.0	1.0717e-12

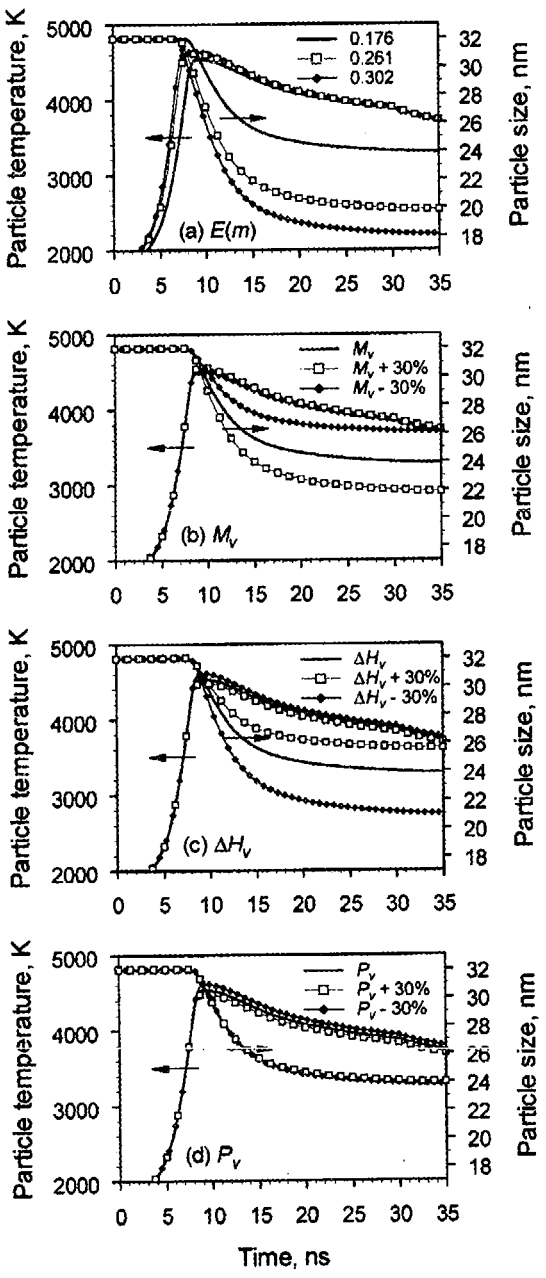

Fig. 1 Uncertainty analysis for specified thermal properties of soot: (*a*) refractive index dependent function; (*b*) mean molecular weight of soot vapor; (*c*) heat of vaporization; and (*d*) vapor pressure.

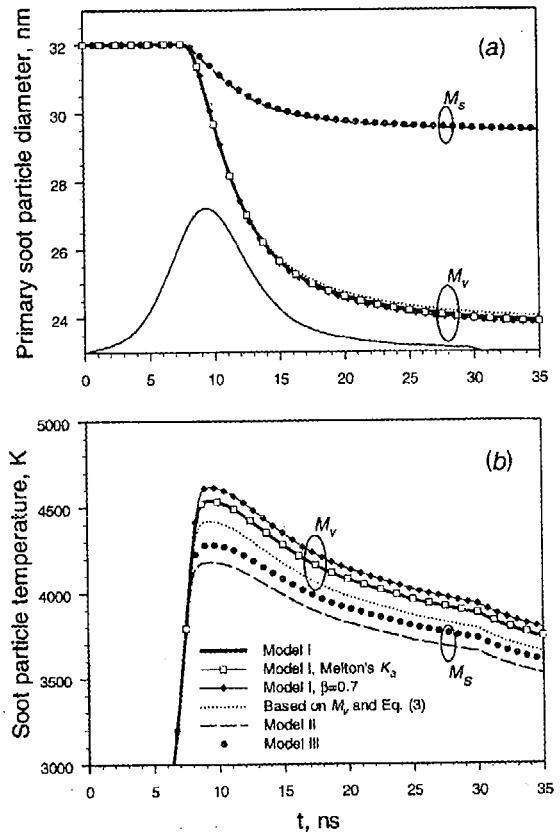

Fig. 2 Effects of some evaporation model parameters and the thermal conductivity on the predicted soot particle size (*a*) and temperature (*b*). The temporal profile of the laser intensity is shown for reference.

evaporation models shown in Table 1 for a laser peak fluence of 0.725 J/cm^2, which is equivalent to a laser pulse energy of 6 mJ for the spatial profile. These results are compared in Fig. 2. Model I predicts that significant soot evaporation occurs under the computational conditions with the particle size reduced by about 26 percent. In contrast, Models II and III predict that the reduction in particle size is only about 8 percent. It is also interesting to observe that Model II predicts the particle size that is only very slightly lower than that from Model III. A slightly smaller particle size starting at the end of laser pulse is noticed as a result of using Melton's K_a since heat conduction loss is underestimated. Use of the incorrect K_a affects the soot temperature only near the end of the laser pulse (30 ns), Fig. 2(*b*), when heat conduction becomes important. Although not demonstrated in Fig. 2, use of Melton's K_a results in an incorrect prediction of the temperature decay at longer times. Results obtained with Model I using $\beta = 0.7$ are also shown in the figure to demonstrate the effect of the evaporation coefficient. To present a thorough picture about the effect of the molecular weight (either M_s or M_v) and the thermal velocity of carbon vapor, equivalent to the mass flux expressions given in Eqs. (2) and (3), results based on M_v and Eq. (3) are also shown in Fig. 2.

Results shown in Fig. 2(*a*) reveal that it is very crucial to employ a molecular weight consistent with the heat of evaporation for the prediction of the soot particle size, while missing a factor of π in the thermal velocity of soot vapor has only slight effect on the particle size (see difference of results between Model II and Model III). Model I employing the incorrect thermal conductivity results in a slightly bigger particle size at the end of the soot evaporation.

Effects of different evaporation models and the evaporation coefficient on the predicted soot temperature are shown in Fig. 2(*b*). Model I predicts that the peak soot temperature is about 4530 K, while Models II and Model III predict about 4177 and 4277 K respectively. The reduced evaporation coefficient, $\beta = 0.7$, reduces the mass loss rate during the first 10 ns of the laser pulse, which can be observed from the slightly slower decreases of soot particle size, Fig. 2(*a*). This reduced mass loss in turn reduces the heat loss through evaporation, resulting in a higher peak soot particle temperature, Fig. 2(*b*). At later times, this increased maximum

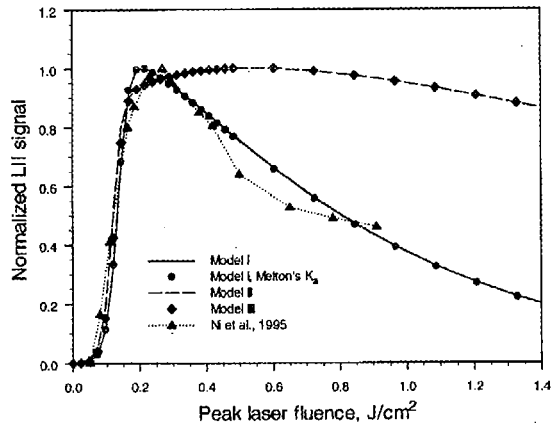

Fig. 3 Variation of the predicted and the experimental normalized prompt LII signals with laser fluence

temperature increases the mass loss rate due to the strong dependence of the vapor pressure on temperature, resulting in a slightly smaller final soot particle size.

It is evident from the results shown in Fig. 2 that the inconsistent use of M_v in the evaporation heat loss term, $\Delta H_v / M_v$, has a far more significant impact on the performance of the model than use of an incorrect expression for the thermal velocity or an inadequate evaporation coefficient. It is interesting to observe from the results shown in Fig. 2(*a*) that parameters that directly alter the mass loss rate of the soot particle, such as the evaporation coefficient β and the thermal velocity, ultimately have an insignificant effect on the soot particle size. Instead, they have a greater effect on the soot temperature. Parameters that directly affect the heat loss rate, such as the molecular weight associated with the heat of evaporation, have far more impact on the results, in particular the soot particle size. The complex interaction of these parameters is due in part to their strong temperature dependencies. The results are indeed a manifestation of the physics of LII: soot temperature is the driving force of soot particle evaporation.

Effects on Excitation Curve. The predicted normalized LII signal at 400 nm (collected at 20 ns after the start of the laser pulse for a gate width 18 ns) are compared in Fig. 3 with the experimental data of Ni et al. [17]. The excitation curve predicted by Model I agrees qualitatively well to the experimental curve, while Models II and III fail to capture the correct shape of the excitation curve.

Conclusions

Numerical results obtained using different evaporation models are presented and compared to demonstrate the importance of the evaporation model to the overall performance of the LII model. The following conclusions are reached based on the numerical results of this study:

1 Use of a molecular weight consistent with the heat of evaporation is crucial to the overall performance of the LII model. When a correct molecular weight based on the carbon vapor is used, the LII model predicts the excitation curve for prompt LII signal collected at a fixed duration in qualitative agreement with experimental observation.

2 The incorrect use of the molecular weight for solid carbon associated with the heat of evaporation drastically affects the results of the model prediction. It results in lower soot temperature and significantly less soot evaporation. It also fails to predict the correct shape of the excitation curve.

3 The incorrect expression for the thermal velocity of carbon vapor affects the model results significantly less than the effect of the incorrect molecular weight.

The present study by no means attempts to claim that the correct formulation presented for the state-of-the-art evaporation model is adequate and truly reflects the soot evaporation process under intense evaporation. The emphasis of this work is that the current evaporation model must be used correctly in the evaluation of the LII model against experimental data.

References

[1] Eckbreth, A. C., 1977, "Effects of Laser-Modulated Particulate Incandescence on Raman Scattering Diagnostics," J. Appl. Phys., **48**, pp. 4473–4479.

[2] Melton, L. A., 1984, "Soot Diagnostics Based on Laser Heating," Appl. Opt., **23**, pp. 2201–2208.

[3] Dasch, C. J., 1984, "New Soot Diagnostics in Flames Based on Laser Vaporization of Soot," *Twentieth Symposium (International) on Combustion*, The Combustion Institute, pp. 1231–1237.

[4] Tait, N. P., and Greenhalgh, D. A., 1993, "PLIF Imaging of Fuel Fraction in Practical Devices and LII Imaging of Soot," *Berichte der Bunsengesellschaft fuer Physikalische Chemie*, **97**, pp. 1619–1625.

[5] Hofeldt, D. L., 1993, "Real-Time Soot Concentration Measurement Technique for Engine Exhaust Streams," Society of Automotive Engineers, SAE Paper No. 930079.

[6] Mewes, B., and Seitzman, J. M., 1997, "Soot Volume Fraction and Particle Size Measurements with Laser-Induced Incandescence," Appl. Opt. **36**, pp. 709–717.

[7] Snelling, D. R., Smallwood, G. J., Campbell, I. G., Medlock, J. E., and Gülder, O. L., 1997, "Development and Application of Laser-Induced Incandescence (LII) as a Diagnostic for Soot Particulate Measurements," *Advanced Non-Intrusive Instrumentation for Propulsion Engines*, AGARD Conference Proceedings 598, pp. 23-21 to 23-29.

[8] McManus, K. R., Frank, J. H., Allen, M. G., and Rawlins, W. T., 1998, "Characterization of Laser-Heated Soot Particles Using Optical Pyrometry," AIAA Paper No. 98-0159.

[9] Will, S., Schraml, S., Bader, K., and Leipertz, A., 1998, "Performance Characteristics of Soot Primary Particle Size Measurements by Time-Resolved Laser-Induced Incandescence," Appl. Opt., **37**, pp. 5647–5658.

[10] Snelling, D. R., Liu, F., Smallwood, G. J., and Gülder, O. L., 2000, "Evaluation of the Nanoscale Heat and Mass Transfer Model of the Laser-Induced Incandescence: Prediction of the Excitation Intensity," *Thirty Fourth National Heat Transfer Conference*, NHTC2000-12132.

[11] Schraml, S., Dankers, S., Bader, K., Will, S., and Leipertz, A., 2000, "Soot Temperature Measurements and Implications for Time-Resolved Laser-Induced Incandescence (Tire-LII)," Combust. Flame, **120**, pp. 439–450.

[12] Leider, H. R., Krikorian, O. H., and Young, D. A., 1973, "Thermodynamic Properties of Carbon up to the Critical Point," Carbon, **11**, pp. 555–563.

[13] Kennard, E. H., 1938, *Kinetic Theory of Gases*, McGraw Hill Book Company, New York, pp. 63–69.

[14] Tsederburg, N. V., 1965, *Thermal Conductivity of Gases and Liquids*, The M.I.T Press, Cambridge, MA, p. 89.

[15] Lee, S. C., and Tien, C. L., 1981, "Optical Constants of Soot in Hydrocarbon Flames," *Eighteenth Symposium (International) on Combustion*, The Combustion Institute, pp. 1159–1166.

[16] Chase, M. W., Jr., Davies, C. A., Downey, J. R., Jr., Frurip, D. J., McDonald, R. A., and Syverud, A. N., 1985, "JANAF Thermochemical Tables," Third Edition, Journal of Physical and Chemical Reference Data, **14**, Suppl. 1.

[17] Ni, T., Pinson, J. A., Gupta, S., and Santoro, R. J., 1995, "Two-Dimensional Imaging of Soot Volume Fraction by the Use of Laser-Induced Incandescence," Appl. Opt., **34**, pp. 7083–7091.